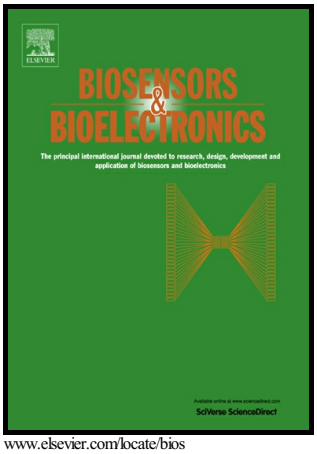

www.elsevier.com/locate/bios

Fabricating photoelectrochemical aptasensor for selectively monitoring microcystin-LR residues in fish based on visible light-responsive BiOBr nanoflakes/N-doped graphene photoelectrode

Xiaojiao Du, Ding Jiang, Liming Dai, Lei Zhou, Nan Hao, Jing Qian, Baijing Qiu, Kun Wang

PII: S0956-5663(16)30190-7
DOI: http://dx.doi.org/10.1016/j.bios.2016.02.072
Reference: BIOS8508

To appear in: *Biosensors and Bioelectronic*

Received date: 9 January 2016
Revised date: 24 February 2016
Accepted date: 29 February 2016

Cite this article as: Xiaojiao Du, Ding Jiang, Liming Dai, Lei Zhou, Nan Hac Jing Qian, Baijing Qiu and Kun Wang, Fabricating photoelectrochemica aptasensor for selectively monitoring microcystin-LR residues in fish based o visible light-responsive BiOBr nanoflakes/N-doped graphene photoelectrode *Biosensors and Bioelectronic,* http://dx.doi.org/10.1016/j.bios.2016.02.072

Fabricating photoelectrochemical aptasensor for selectively monitoring microcystin-LR residues in fish based on visible light-responsive BiOBr nanoflakes/N-doped graphene photoelectrode

Xiaojiao Du[a1], Ding Jiang[b1], Liming Dai[a], Lei Zhou[a], Nan Hao[a], Jing Qian[a], Baijing Qiu[a], Kun Wang[a*]

[a]Key Laboratory of Modern Agriculture Equipment and Technology, School of Chemistry and Chemical Engineering, Jiangsu University, Zhenjiang, 212013, P.R. China

[b]School of Food and Biological Engineering, Jiangsu University, Zhenjiang, 212013, P.R. China

*Corresponding author. Tel.: +86 511 88791800; fax: +86 511 88791708. E-mail address: wangkun@ujs.edu.cn

ABSTRACT

The presence of microcystins in fish has been augmenting the risk of toxicity to animal and human health. Herein, a selective and sensitive method for detecting microcystin-LR (MC-LR) in fish samples by integrating the photoelectrochemical (PEC) technique and the specific recognition ability of aptamer was developed. Specifically, as an efficient PEC transducer, the BiOBr nanoflakes/N-doped graphene p−n heterojunction electrode was utilized as the aptamer immobilization platform via the π–π stacking interaction, which would be a biosensor enabling the convenient and exquisite PEC analysis. Subsequently, the PEC response of constructed aptasensor was specific binding to MC-LR. Other isoforms did not

[1] These authors contributed equally to this work.

interfere with the detection process, and thus, it could be applied for the highly selective determination of MC-LR level. Under the optimized condition, the PEC signal versus the logarithm of the MC-LR concentration was in good linear relationship ranging from 0.1 pM to 100 nM with detection limit about 0.03 pM. The constructed method was employed to analyze fish samples collected from the local supermarket. The overall analytical recovery of MC-LR in the fish matrices ranged from 97.8 to 101.6 %, with relative standard deviation (RSD) of 2.52~5.14 %, implying it would have great potential in farm product analysis.

Keywords: BiOBr nanoflakes; N-doped graphene; p-n heterojunction; Photoelectrochemical; Aptasensor; Microcystin-LR

1. Introduction

Microcystins (MCs) are a known group of cyclic peptide hepatotoxins and tumor promoters produced by freshwater cyanobacteria (Eissa et al., 2014; Li et al., 2014). Among this family, microcystin-LR (MC-LR) is the most common and toxic variant (Eissa et al., 2014). MC-LR contains leucine (L) and arginine (R) at the two variable positions, which is the firstly chemically identified and widely studied microcystin (Eissa et al., 2014). Acute or chronic exposure to MC-LR-contaminated drinking water or agriculture products can cause liver failure in animals and human and may even lead to death (Carmichael, 1992; Poste et al., 2011). Especially, it has been established that fish consumption may be dominant source of microcystin exposure for humans recently (Poste et al., 2011). Consequently, there is an urgent need for monitoring MC-LR in fish samples to protect the public health.

Considering that more than 80 isoforms of MCs have been identified, it is hard to discriminate these structurally similar microcystin congeners, and their performances are limited by the high matrix effect when developing sensitive and specific methods for detecting MC-LR (Eissa et al., 2014). Many analytical techniques have been utilized for MC-LR detection, including chromatography (Falconer, 1993), liquid chromatography/mass spectrometry (LC-MS) (Li et al., 2014), capillary electrophoresis (Bateman et al., 1995), Raman spectroscopy (Saito et al., 2008), and protein phosphatase inhibition assays (Ma et al., 2009; Zhang et al., 2010a). Whereas these methods provide good sensitivity, they usually require highly qualified personnel, bulky apparatus, high cost, and time-consuming process.

Electrochemical technique, a rather effective mean with fast response and high sensitivity, has raised extensive attention over the past decades (Zhang et al., 2010b). It is simpler in equipment and easier to implement on-line monitoring compared with those apparatus-involved methods. However, to our best knowledge, MC-LR is chemically inert, making it difficult to be detected via direct electrochemical reduction or oxidation (Ma et al., 2009; Chen et al., 2012). In the past several decades, the photoelectrochemical (PEC) method has been considered to be a more sensitive technique ascribing combination of electrochemical and optical technique, not only possessing the superiority of electrochemical technique but also an ultrasensitive capacity due to the different forms of energy for excitation (light) and detection (current) (Chen et al., 2012). Recent studies showed the BiOBr photocatalyst had remarkable ability to promote the oxidative decarboxylation of MC-LR and decarboxylate the free acid groups on D-glutamic acid (Glu) and methyl-D-aspartic acid (MeAsp) in the photocatalytic degradation (Fang et al., 2011; Wang et al., 2015). As a result, it is regarded to be a convenient and fast analytical method for PEC sensing MC-LR by exploiting the photocatalytic oxidation of MC-LR in the presence of the BiOBr catalyst. Nevertheless, the PEC method lacks selectivity since its high oxidation potential.

In the past few years, immunoassay and molecularly imprinted polymers (MIPs) techniques have been introduced into PEC sensing system in order to overcome above limitations (Chen et al., 2012; Tian et al., 2012). Although having been adopted to obtain good selectivity towards MC-LR, they are still costly due to

the required antibody and/or instruments and time-consuming with complicated fabrication methodologies, respectively, and hence not suitable for onsite analysis (Neves et al., 2015). Aptamers, as well-known antibody mimetics with high specificity and affinity to specific targets, have been widely utilized to establish highly selective biosensors, coupling with optical, mass, thermal and electrochemical transducers, which are capable of recognizing their targets with high specificities and affinities often matching or even exceeding those of antibodies (Liu et al., 2015; Jenison et al., 1994; Ocaña et al., 2015). Particularly, DNA aptamers have some pivotal advantages over antibodies, such as a comparatively smaller size, a cheap synthesis, an in vitro selection process, an increased resistance to degradation, and reversible denaturation (Neves et al., 2015). Besides, the MIPs technique suffers complex fabrication process and experienced professionals. As a consequence, it's predictable that aptamer-based assays may provide an alternative avenue to alleviate some of the drawbacks of existing detection technologies. At present, almost no efforts have been devoted to the application of MC-LR aptamers as biocomponents in PEC bioanalysis. Therefore, it's essential to develop new, rapid, cheap and selective PEC aptasensors for MC-LR detection in different matrices.

Herein, a simple and selective PEC protocol by integrating the specific recognition ability of aptamer was designed for MC-LR sensing in fish samples. In particular, we pioneered the BiOBr nanoflakes/N-doped graphene (BiOBrNFs-NG) nanocomposites p−n heterojunction on indium tin oxide (ITO) electrode as a visible light-responsive material, which was chosen to immobilize the aptamer via π–π

stacking interactions. Furthermore, the aptamer modified BiOBrNFs-NG electrode was applied for the highly selective quantification of MC-LR level, on the strength of the specific recognition ability between aptamer and MC-LR, which was suitable for routine analysis of fish samples.

2. Experimental

2.1. Reagents

Microcystin-LA (MC-LA), microcystin-YR (MC-YR) and microcystin-LR (MC-LR) were purchased from J&K Chemical Ltd. (Shanghai). The DNA oligonucleotides (single-strand DNA (ssDNA) aptamer of MC-LR) were synthesized by Sangon Biotech Co., Ltd. (Shanghai, China) and used without further purification with the sequence of 5'-GGC GCC AAA CAG GAC CAC CAT GAC AAT TAC CCA TAC CAC CTC ATT ATG CCC CAT CTC CGC-3'. Tris (hydroxymethyl) aminomethane (Tris) and ethylenediaminetetraacetic acid disodium salt (EDTA) were obtained from Aladdin (Shanghai, China). Standard MCs samples were dissolved in binding buffer (50 mM Tris–HCl, pH 7.4, 0.1 M NaCl, 5 mM $MgCl_2$, 0.2 M KCl and 1.0 mM EDTA) to obtain various concentrations of MCs. The DNA aptamer solution was prepared by dissolving DNA in the binding buffer. All solutions were prepared using Milli-Q grade water (Millipore water purification system $\geqslant$18 MΩ, Milli-Q, Millipore, Billerica, MA). All the reagents were used as received.

2.2. Apparatus

Transmission electron microscope (TEM) images were recorded with a

JEM-2010 high-resolution TEM system (JEOL, Japan) performed at an accelerating voltage of 200 kV and the phase characterization was operated by X-ray diffraction (XRD) using a D8 advance diffractometer system equipped with Cu Kα radiation (Bruker Co., Germany). Raman spectra were carried out on a RM 2000 microscopic confocal Raman spectrometer (Renishaw, UK). X-ray photoelectron spectrometry (XPS) analyses were recorded on an ESCALAB MKII X-ray photoelectron spectrometer. The UV−vis diffuse reflection spectra were acquired for the dry-pressed disk samples utilizing a Scan UV−vis spectrophotometer (UV−vis DRS: UV-2450, shimadzu, Japan) equipped with an integrating sphere assembly with $BaSO_4$ as reflectance sample.

PEC currents measurements and electrochemical impedance spectroscopy (EIS) were performed by a CHI 660B electrochemical workstation (Shanghai Chenhua Instrument Co. Ltd., China) in a standard three−electrode cell system with the ITO as the photoanode, a platinum (Pt) wire as the counter electrode, and a saturated calomel electrode (SCE) as the reference electrode. All the PEC measurements were carried out in 0.1 M phosphate buffer solution (PBS) at 0 V and a 500 W Xe lamp (CHF-XM35-500W, Beijing Chang tuo) was utilized as the visible light source with an intensity (passing through a 400 nm UV-cut filter) of 100 mW cm^{-2}. Current-time (I-t) method was used for the whole PEC experiments. EIS was performed in the 0.1 M KCl solution containing 5 mM $[Fe(CN)_6]^{3-/4-}$ with a frequency from 10^{-1} to 10^5 Hz at a constant potential of 0.23 V.

2.3. The synthesis of BiOBrNFs-NG nanocomposites

The BiOBrNFs-NG nanocomposites were prepared via a facile wet-chemical process. First, NG was synthesized by annealing the resulting mixture after GO and glycine homogeneous mixing at 500 ^{o}C for 2 h under argon atmosphere according to our previous report (Jiang et al., 2015). Next, the BiOBrNFs-NG nanocomposites was synthesized as follows: 0.13 g $Bi(NO_3)_3 \bullet 5H_2O$ was dissolved in 50 mL water (adjusting to pH=3 by adding HNO_3). 3.853 mg NG was dispersed in 50 mL CTAB solution (8×10^{-3} mol/L). Subsequently, the $Bi(NO_3)_3 \bullet 5H_2O$ solution was dropwise added into NG suspension, which was stirred and heated in water bath at 80 ^{o}C for 3 h. After completing the reaction, the precipitate was washed by absolute ethanol and deionized water for 3 times and transferred to oven to dry at 60 ^{o}C for 24 h. The BiOBrNFs-graphene (BiOBrNFs-GR) nanocomposites were synthesized via the same method without adding glycine.

2.4. Stepwise fabrication and detection process of photoelectrochemical aptasensor

The construction of MC-LR PEC aptasensor was illustrated by Scheme 1B. Prior to the preparation of modified ITO electrodes, the basal ITO substrates were placed in boiling water containing 1 M NaOH for 30 min and then were cleaned by ultrasonication in distilled water and ethanol, subsequently. 2 mg mL^{-1} BiOBrNFs-NG suspension was prepared by dispersing 2.0 mg BiOBrNFs-NG in 1.0 mL dimethyl formamide (DMF) with ultrasonic agitation for about 15 min. Immediately following, the ITO surface was coated with 20 microliters BiOBrNFs-NG suspension with insulating glue and an area of 1×0.5 cm^{-2} and dried at under an infrared lamp to obtain BiOBrNFs-NG modified ITO

(BiOBrNFs-NG/ITO). For comparison, solitary BiOBrNFs modified ITO (BiOBrNFs/ITO) and BiOBrNFs-GR modified ITO (BiOBrNFs-GR/ITO) were also prepared in the same procedure. To fabricate the MC-LR biosensor, 15 microliters of 5 μM aptamer was dropped onto the BiOBrNFs-NG/ITO. The aptamer-modified electrodes were dried in ambient air and rinsed with deionized water to remove the excess nonadsorbed aptamer. For a control experiment, the mismatched DNA sequence sensor was fabricated with the same process except replacing the aptamer with the mismatched DNA sequence. 20 microliters of MC-LR of the target concentration in binding buffer was incubated on the aptamer-modified ITO electrodes at room temperature for 30 min and then the electrodes were subsequently washed with binding buffer solution and subjected to PEC measurements.

2.5. Preparation of fish tissues and extraction procedure for MC-LR detection

For measuring MC-LR content in fresh tissue/organ, the fish samples were purchased from a local supermarket of Zhenjiang, China. Before extraction, individual fish was separated from the skin and bones, and then minced, crushed and homogenized by a blender before further treatment (Scheme 1A). The extraction method used in this study was following the protocol reported previously (Eissa et al., 2012; Moreno et al., 2005). An accurately weighed 5.0 g of homogenized tissue or 5.0 g of spiked sample (blank tissue sample was spiked with MC-LR at different mass ratios indicated in the Table 1) was placed into a 10 mL Teflon centrifuge tube, methanol was added and the mixture completely was blended at 1800 rpm for 5 min. The resultant solution was centrifuged twice at 4000 rpm for 10 min. The

supernatant was collected, and the residue was re-extracted. Finally, the supernatant was passed through 0.45 μm cutoff Whatman nylon membrane filters and diluted 1:10 in binding buffer.

2.6. Fish samples measurement

The accuracy of the MC-LR measurements in fish extracts was estimated by calculating the recovery of MC-LR in a standard addition method. The spiked samples were incubated for 30 min with the prepared aptasensor at ambient temperature and the PEC signals were recorded.

3. Results and discussion

3.1. Characterization of BiOBrNFs-NG nanocomposites

The as-synthetized BiOBrNFs-NG nanocomposites were characterized by TEM and XRD (Fig. 1). Fig. 1A showed the TEM image of BiOBrNFs-NG nanocomposites. It can be seen the wrinkle two-dimensional structure of NG sheets. The typical TEM images revealed that BiOBrNFs with hundreds of nanometers in width randomly dispersed on the two-dimensional NG sheets. As presented in Fig. 1B, all of the power XRD peaks of BiOBrNFs could be indexed to a tetragonal phase of BiOBr with lattice constants of a=3.915, c=8.076 (JCPDS Card No. 73-2061) (Ai et al., 2011; Ye et al., 2013). The Raman absorption spectra of the resulting samples as shown in Fig. 1C, the strong peak at around 110 cm^{-1} could be attributed to A_{1g} internal Bi–Br stretching mode, the band at about 150 cm^{-1} would be assigned to the E_g internal Bi–Br stretching mode and the E_g and B_{1g} bands at about 384 cm^{-1} was generated by vibration of Bi–O chemical bonds in BiOBr (Zhang et al., 2013; Tu et

al., 2012), which were observed in the Raman spectra of both the solitary BiOBrNFs and BiOBrNFs-NG nanocomposites. Moreover, the BiOBrNFs-NG nanocomposites displayed two relatively obvious peaks at 1358 and 1588 cm^{-1}, corresponding to the D band and G band of NG (Jiang et al., 2015), respectively. To verify successful nitrogen element doping and chemical nature of the as-prepared samples, XPS analysis was investigated. As illustrated in Fig. 1D, the wide range scan XPS spectrum of BiOBrNFs-NG confirmed the four elements (Bi, Br, C and O) in the nanocomposites (Zhang et al., 2013). More importantly, a marked N 1s binding energy peak was observed (inset of Fig. 1D) at the BiOBrNFs-NG nanocomposites except for the four elements (Jiang et al., 2015), demonstrating doping nitrogen successfully. All the results proved that the prepared sample was the BiOBrNFs-NG nanocomposites.

Fig. S1 showed the UV–vis diffuse reflectance spectra of the solitary BiOBrNFs, BiOBrNFs-GR and BiOBrNFs-NG nanocomposites. According to the equation (E_g=1240/λ), extrapolating the linear part of curve gave an indirect band gap of 2.80 eV, suggesting BiOBrNFs was responsive to visible light, while there was an evident enhanced absorbance in the visible-light region from 400 to 800 nm for BiOBrNFs-GR and BiOBrNFs-NG nanocomposites (Zhang et al., 2010c; Wang et al., 2014). This result may be attributed to that the presence of GR and NG resulted in reduced reflection of light and thus enhanced absorption in the visible-light region (Zhang et al., 2010c; Wang et al., 2014). The enhanced light absorption led to the generation of more electron–hole pairs under the same visible

light irradiation, which subsequently could lead to a higher photocatalytic activity (Xia et al., 2014). Therefore, the introduction of GR and NG would likely enhance the activity of visible-light responsive BiOBr photoactive materials. Besides, compared with the BiOBrNFs-GR nanocomposites, the BiOBrNFs-NG nanocomposites exhibited a notable red-shift in the absorption edge and further extended the absorbance to the visible region, implying the BiOBrNFs-NG nanocomposites would show more excellent PEC performances.

3.2. Characterization and photocurrent behaviors of the modified photoactive electrodes

In order to investigate the photoinduced behavior of different modified electrodes, the photocurrent responses of BiOBrNFs/ITO, BiOBrNFs-GR/ITO and BiOBrNFs-NG/ITO electrodes under the visible light illumination were explored (Fig. 2A). The solitary BiOBrNFs could be effectively activated under visible light, resulting in a weak photocurrent response of 88.7 nA (curve a). The photocurrent of the BiOBrNFs-NG/ITO electrode was about 4.6 times that of BiOBrNFs/ITO electrode (curve c) and near 2 times that of the BiOBrNFs-GR/ITO electrode (curve b). That might be attributed to that NG has a more enhanced charge transfer rate to facilitate the efficient electron–hole separation and suppress the rapid recombination of electrons and holes than GR (Wang et al., 2014; Mou et al., 2014). Besides, another reason could be elaborated that the formation of p-n heterojunction between BiOBrNFs and NG in the nanocomposites promoted more effective charge separation and thus an increased photocurrent (Chang et al., 2014). The improved

charge separation effect can be confirmed by the EIS. As depicted in Fig. 2B, NG possessed the smallest curvatures of impedance arcs in the plot as compared to the other two counterparts and thus could accelerate the photoelectron-transfer and led to increasing the photocurrent (Mou et al., 2014).

To verify the successful assembly of BiOBrNFs-NG and aptamer on the electrodes as expected, the EIS characterization was performed on the ITO electrode. Fig. 2C displayed the impedance spectra from different modified electrodes related to each construction step of this biosensor. With the aptamer assembled on BiOBrNFs-NG/ITO electrode (curve b), charge-transfer resistance (Rct) increased significantly from 23.6 to 285.7 Ω, implying the DNA aptamer was successfully coated on the BiOBrNFs-NG surface via π–π stacking interactions between the NG hexagonal cells and the nucleobases of the DNA. After the aptasensor having specific reaction with 1 nM MC-LR, the diameter of the semicircle (curve c) became smaller than curve b due to the complex formation change on the electrode surface (Lin et al., 2013). All these results confirmed the effective immobilization of the aptamer on BiOBrNFs-NG modified electrode via π–π stacking interaction and the target analyte MC-LR had specific binding to the aptamer.

The PEC aptasensor construction procedure and the mechanism for the PEC detection of MC-LR were illustrated in Scheme 1B. When the MC-LR molecules were present, the aptamer immobilized on BiOBrNFs-NG electrode could specifically and sensitively capture MC-LR molecules on the surface of biosensor rather than the release of the aptamer from graphene surface upon protein−aptamer

binding (Eissa et al., 2014), which was consistent with the conclusion from EIS. The PEC results demonstrated that, with incubating the aptasensor in the solution of MC-LR, the photocurrent of the aptasensor was enhanced markedly compared to that of in blank PBS, shown by Fig. 2D, suggesting the feasibility of the constructed biosensor for detecting the MC-LR.

The MCs are readily oxidized by the catalyst BiOBr in the photocatalytic degradation (Fang et al., 2011; Wang et al., 2015), in which the BiOBr catalyst had remarkable ability to promote the oxidative decarboxylation of MC-LR. As a result, the tentative mechanism for the generation of enhanced photocurrent for MC-LR on the PEC biosensor was that the captured MC-LR molecules on the biosensor interface were quickly oxidized by the photoinduced holes of BiOBr the and the recombination of photoinduced electrons and holes was retard (Scheme 1B). Therefore, an amplified photocurrent was obtained in the presence of MC-LR.

3.3. Optimization of conditions for photoelectrochemical aptasensor

To fabricate the efficient and ultrasensitive PEC aptasensor, it is essential to optimize important parameters involved in the biosensor fabrication process and MC-LR detection process. The immobilization time between aptamer and BiOBrNFs-NG nanocomposites had a great effect on the performances of the proposed biosensor. As illustrated in Fig. S2A, the photocurrent decreased with the increase of time. When it reached 0.5 h, the photocurrent had reached a plateau, it meant that the surface of the electrode had been fully covered by the aptamer or reached saturation. As a result, 0.5 h was enough and selected as the immobilization

time in the following experiment. As displayed in Fig. S2B, the PEC response toward MC-LR markedly increased with increasing the aptamer concentration up to 3 μM, indicating that higher concentration of aptamer immobilized on the electrode surface could capture more MC-LR molecules, while the aptamer concentration exceeded 3 μM, the PEC response tended to decay. This phenomenon could be explained by the steric hindrance generated by excessive aptamer, resulting in the blockage of electrons transfer and poor PEC response (Liu et al., 2015). Therefore, 3 μM was the saturated concentration of the DNA aptamer and was chosen to be the optimized concentration of the aptamer. The binding time of MC-LR with its aptamer is another important factor that affected the fabrication of the aptasensor. In consequence, the influence of the binding time of MC-LR with its aptamer was also investigated. As shown in Fig. S2C, it was vividly described that the PEC response toward MC-LR distinctly increased with the increasing binding time from 5 to 20 min and then reached a stationary region in 30 min. Thus, 30 min was selected as the optimal binding time between the sensing interfaces with MC-LR molecules in this research.

The effects of pH value in PBS on the photocurrent response of the aptamer-DNA/BiOBrNFs-NG/ITO electrode after interacting with 1 nM MC-LR were evaluated for the optimal condition. From Fig. S2D, the photocurrent of the PEC aptasensor reached the maximum at pH 7.4, which was measured in PBS with different pH ranging from 4.0 to 9.0. Hence, PBS with the pH value of 7.4 was exploited in subsequent studies.

3.4. Analytical performances of PEC aptasensor

Based on the "signal-on" strategy, the constructed aptasensor was employed to the MC-LR determination as stated above. Fig. 3A displayed the PEC responses of aptamer-DNA/BiOBrNFs-NG/ITO electrodes to MC-LR at different concentrations. The photocurrent response increased with increasing the concentrations of MC-LR, which was attributed to capturing more MC-LR molecules involved the PEC process. This biosensor was found to be linearly proportional to the logarithm of MC-LR concentration ranging from 0.1 pM to 100 nM with a correlation coefficient of 0.999 (Fig. 3B). The limit of detection (LOD) was estimated to be 3.3×10^{-2} pM (defined as S/N=3), which was one order lower than the aptamer-based assay method reported previously (Eissa et al., 2014; Lin et al., 2013; Wang et al., 2015).

3.5. Interference study, and reproducibility of the PEC aptasensor

To evaluate the specificity of the PEC aptasensor, control experiments were performed by measuring the photocurrent response change of the aptasensor in the case of two structure similar molecules (MC-LA and MC-YR) from other microcystin congeners and a control DNA. Significant photocurrent change was obtained only in the presence of MC-LR, this meant that this aptasensor was only responsive to MC-LR and did not show cross-reactivity with structurally similar MC-YR and MC-LA. To rule out the possibility of the nonspecific adsorption of MCs on the NG sheets, a control experiment was also conducted using non specific DNA sequence immobilized on the BiOBrNFs-NG/ITO using the identical protocol and incubated with 1 nM MC-LR. We didn't see any significant change in the

photocurrent response (Fig. 3), suggesting that none of these substances would interfere with the quantification of MC-LR.

The stability and repeatability of the proposed biosensor was also measured by detecting the photocurrent response data of the different modified electrodes at the same concentration of MC-LR (1 nM). The relative standard deviation (RSD) of the resulting photocurrent density was 3.46 % (n=5), indicating that the proposed sensing interface had good reproducibility and could be applied in real sample detection. The investigation of the repeatability was performed by the recovery of photocurrent response at 1 nM MC-LR, the results demonstrated that the aptasensor could be regenerated at least five times with the RSD of 7.6 %. The aptamer/BiOBrNFs-NG/ITO electrode after storage at 4 ^{o}C did not have obvious change in photocurrent response after two weeks, suggesting the high stability and detection reliability of the sensor.

3.6. Application in fish samples

The proposed method was evaluated using a series of fish samples (uncontaminated and spiked fish samples) with MC-LR. No MC-LR at detectable levels was found in fish samples. The accuracy of the method was expressed as recovery rate by analyzing blank samples spiking with different standard MC-LR indicated in Table 1. A good recovery percentage in the range of 97.8~101.6 % with the RSD of 2.52~5.14 % was obtained for the spiked fish extract, implying a nonsignificant effect of the fish matrix on this aptasensor. Therefore, the PEC aptamer-based assay method could be satisfactorily applied to the quantification of

the MC-LR in real fish samples.

4. Conclusion

In summary, a novel, selective and sensitive method for the quantification of trace levels of MC-LR from fish samples was proposed based on coupling the high-performance PEC technique with highly specific aptamer. The BiOBrNFs-NG nanocomposites were used as the photoelectrode to develop a novel PEC biosensor for highly selective detection of MC-LR. The high recovery verified that this method was valid for the analysis of MC-LR in fish samples.

Acknowledgment

This work was supported by the National Natural Science Foundation of China (Nos. 21375050, 21405063 and 21505055), the Natural Science Foundation of Jiangsu province (No. BK20150486), a project funded by the Priority Academic Program Development of Jiangsu Higher Education Institutions (No. PAPD-2014-37), the Jiangsu Province Synergistic Innovation Center Program of Modern Agricultural Equipment and Technology (No. NZXT01201403), Qing Lan Project and China Postdoctoral Science Foundation funded project (2015T80517).

References

Ai, Z.H., Ho, W.K., Lee, S.C., 2011. J. Phys. Chem. C 115, 25330–25337.

Bateman, K.P., Thibault, P., Douglas, D.J., White, R.L., 1995. J. Chromatogr., A 712, 253−268.

Carmichael, W.W.J., 1992. Appl. Bacteriol. 72, 445−459.

Chang, C., Zhu, L.Y., Wang, S.F., Chu, X.L., Yue, L.F., 2014. ACS Appl. Mater. Interfaces 6, 5083−5093.

Chen, K., Liu, M.C., Zhao, G.H., Shi, H.J., Fan, L.F., Zhao, S.C., 2012. Environ. Sci. Technol. 46, 11955–11961.

Eissa, S., Ng, A., Siaj, M., Zourob, M., 2014. Anal. Chem. 86, 7551–7557.

Eissa, S., Zourob, M., 2012. Nanoscale 4, 7593−7599.

Falconer, I.R., 1993. In Algal Toxins in Seafood and Drinking Water. Ed.; Academic Press: London 165−175.

Fang, Y.F., Huang, Y.P., Yang, J., Wang, P., Cheng, G.W., 2011. Environ. Sci. Technol. 45, 1593–1600.

Jenison, R.D., Gill, S.C., Pardi, A., Polisky, B., 1994. Science 263, 1425–1429.

Jiang, D., Du, X.J., Liu, Q., Zhou, L., Qian, J., Wang, K., 2015. ACS Appl. Mater. Interfaces 7, 3093−3100.

Li, Y.W., Zhan, X.J., Xiang, L., Deng, Z.S., Huang, B.H., Wen, H.F., Sun, T.F., Cai, Q.Y., Li, H., Mo, C.H., 2014. J. Agric. Food Chem. 62, 11831–11839.

Lin, Z.Y., Huang, H.M., Xu, Y.X., Gao, X.Y., Qiu, B., Chen, X., Chen, G.N., 2013. Talanta 103, 371–374.

Liu, Y., Yan, K., Okoth, O.K., Zhang, J.D., 2015. Biosens. Bioelectron. 74, 1016–1021.

Moreno, I.M., Molina, R., Jos, A., Picó, Y., Cameán, A.M., 2005. J. Chromatogr. A 1080, 199–203.

Mou, Z.G., Wu, Y.J., Sun, J.H., Yang, P., Du, Y.K., Lu, C., 2014. ACS Appl. Mater.

Interfaces 6, 13798–13806.

Ma, W., Chen, W., Qiao, R.R., Liu, C.Y., Yang, C.H., Li, Z.K., Xu, D.H., Peng, C.F., Jin, Z.Y., Xu, C.L., Zhu, S.F., Wang, L.B., 2009. Biosens. Bioelectron. 25, 240−243.

Neves, M.A.D., Blaszykowski, C., Bokhari, S., Thompson, M., 2015. Biosens. Bioelectron. 72, 383–392.

Ocaña, C., Hayat, A., Mishra, R.K., Vasilescu, A., Valle, M.D., Marty, J.L., 2015. Bioelectrochem. 105, 72–77.

Poste, A.E., Hecky, R.E., Guildford, S.J., 2011. Environ. Sci. Technol. 45, 5806−5811.

Saito, K., Sei, Y., Miki, S., Yamaguchi, K., 2008. Toxicon 51, 1496−1498.

Tian, J.P., Zhao, H.M., Zhao, H.R., Quan, X., 2012. Microchim. Acta 179, 163–170.

Tu, X.M., Luo, S.L., Chen, G.X., Li, J.H., 2012. Chem. Eur. J. 18, 14359–14366.

Wang, F.F., Liu, S.Z.. Lin, M.X., Chen, X., Lin, S.R., Du, X.Z., Li, H., Ye, H.B., Qiu, B., Lin, Z.Y., Guo, L.H., Chen, G.N., 2015. Biosens. Bioelectron. 68, 475–480.

Wang, S.L., Li, J.J., Zhou, X.D., Zheng, C.C., Ning, J.Q., Zhong, Y.J., Hu, Y., 2014. J. Mater. Chem. A 2, 19815–19821.

Wang, S.L., Wang, L.L., Ma, W.H., Johnson, D.M., Fang, Y.F., Jia, M.K., Huang, Y.P., 2015. Chem. Eng. J. 259, 410–416.

Xia, J.X., Di, J., Yin, S., Li, H.M., Xu, L., Xu, Y.G., Zhang, C.Y., Shu, H.M., 2014. Ceram. Int. 40, 4607–4616.

Ye, L.Q., Liu, J.Y., Jiang, Z., Peng, T.Y., Zan, L., 2013. Appl. Catal., B 142–143, 1–

7.

Zhang, D., Li, J., Wang, Q.G., Wu, Q.S., 2013. J. Mater. Chem. A 1, 8622–8629.

Zhang, J., Lei, J.P., Xu, C.L., Ding, L., Ju, H.X., 2010a. Anal. Chem. 82, 1117−1122.

Zhang, X.R., Zhao, Y.Q., Li, S.G., Zhang, S.S., 2010b. Chem. Commun. 46, 9173–9175.

Zhang, Y.H., Tang, Z.R., Fu, X.Z., Xu, Y.J., 2010c. ACS Nano 4, 7303–7314.

Figure captions

Scheme 1. (A) The pretreatment procedure of fish samples. (B) Schematic diagram of PEC aptasensing principle on the basis of the BiOBrNFs-NG/ITO electrode.

Fig. 1. (A) The typical TEM image of the resulting BiOBrNFs-NG samples. (B) XRD patterns of the solitary BiOBrNFs (a), BiOBrNFs-GR (b) and BiOBrNFs-NG samples (c); (C) Raman spectra of the solitary BiOBrNFs (a) and the as-prepared BiOBrNFs-NG nanocomposites (b); (D) The full scan XPS spectra of BiOBrNFs-NG nanocomposites (Inset: XPS of N 1s peaks of the BiOBrNFs-NG nanocomposites).

Fig. 2. (A) Transient photocurrent response of the BiOBrNFs/ITO (a), BiOBrNFs-GR/ITO (b), BiOBrNFs-NG/ITO (c), and (B) electrochemical impedance spectra of BiOBrNFs/ITO (a), BiOBrNFs-GR/ITO (b), and BiOBrNFs-NG/ITO (c). (C) Impedance spectra of BiOBrNFs-NG/ITO (a), the aptamer-DNA/BiOBrNFs-NG/ITO and after interaction with 1 nM MC-LR (b, c) and (D) the photocurrent curves of the aptamer-DNA/BiOBrNFs-NG/ITO and after interaction with 1 nM MC-LR (a, b).

Fig. 3. (A) Photocurrent responses of aptamer-DNA/BiOBrNFs-NG/ITO electrodes in 0.1 M PBS at a bias potential of 0.0 V (vs SCE) before and after incubation with different concentrations of MC-LR: (a) 0, (b) 0.1, (c) 1, (d) 5, (e) 10, (f) 10^2, (g) 10^3,

(h) 10^4, (i) 5×10^4, (j) 10^5 pM and (B) linear relationship between PEC response of this biosensor and MC-LR concentration. The error bars are the standard error of the method (±SD, n=5).

Fig. 4. Photocurrent response of this aptasensor to 1.0 nM of MC-LR, MC-LA, MC-YR and the control DNA.

Table 1 Determination of MC-LR residue in fish samples (n=5) by the PEC method.

Sample	Spiked (nM)	Found (nM)	Recovery (%)	R.S.D (%)
1	0	0	-	-
2	0.1	0.0991	99.1	3.22
3	1	0.9782	97.8	2.52
4	5	5.0822	101.6	5.14

Scheme 1.

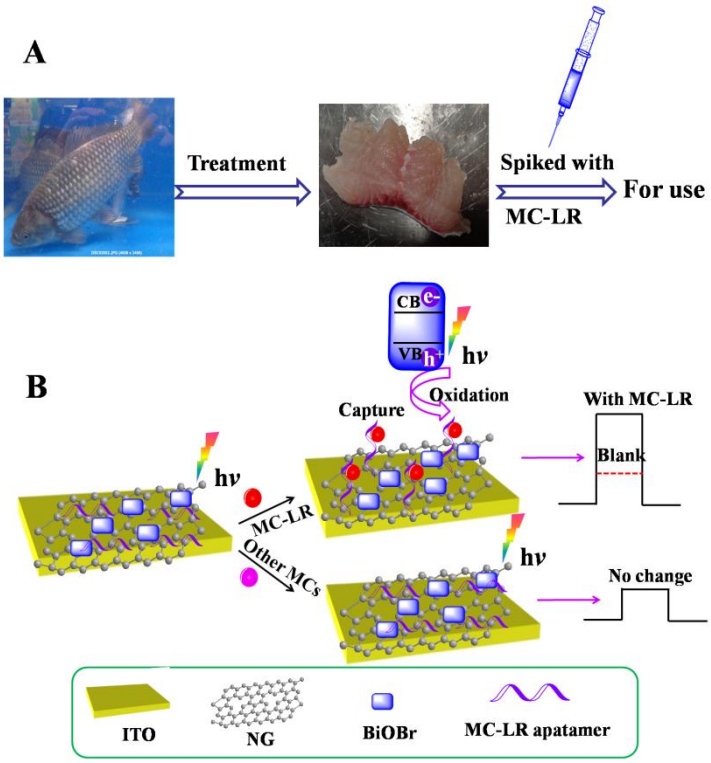

Fig. 1.

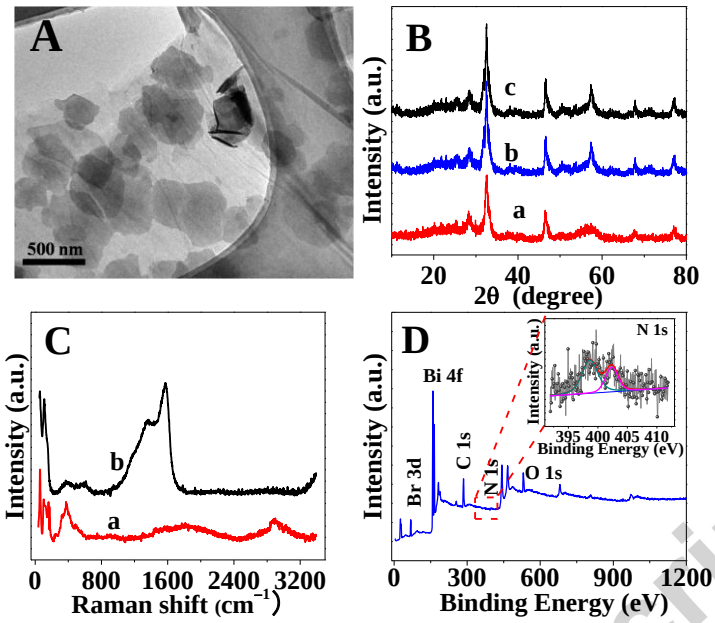

Fig. 2.

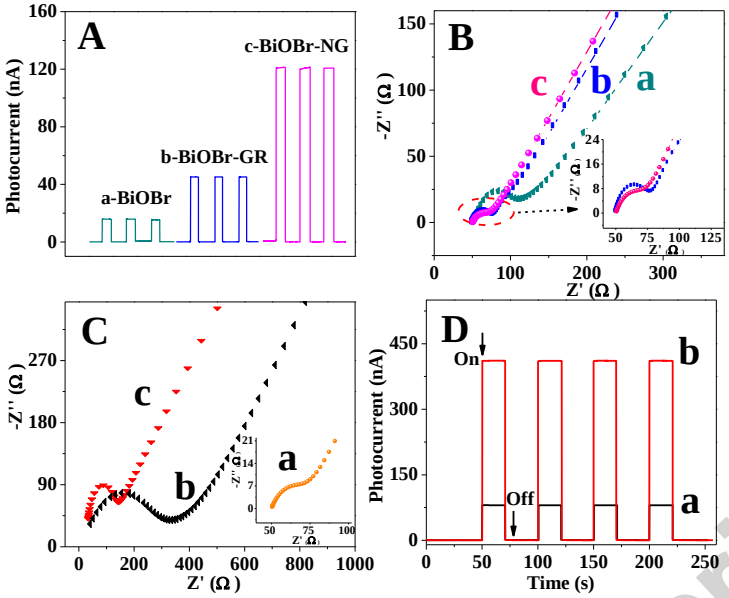

Fig. 3.

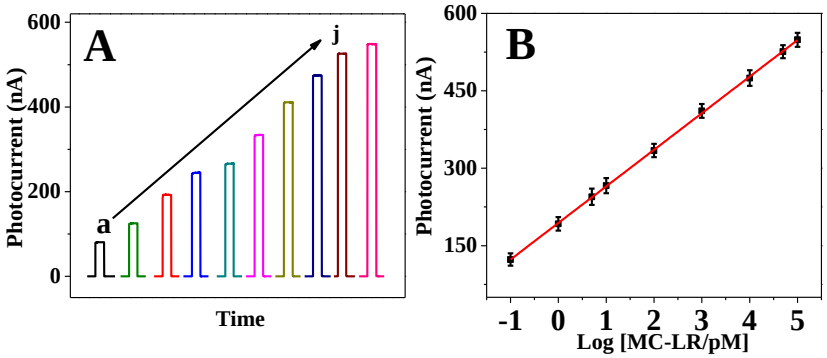

Fig. 4.

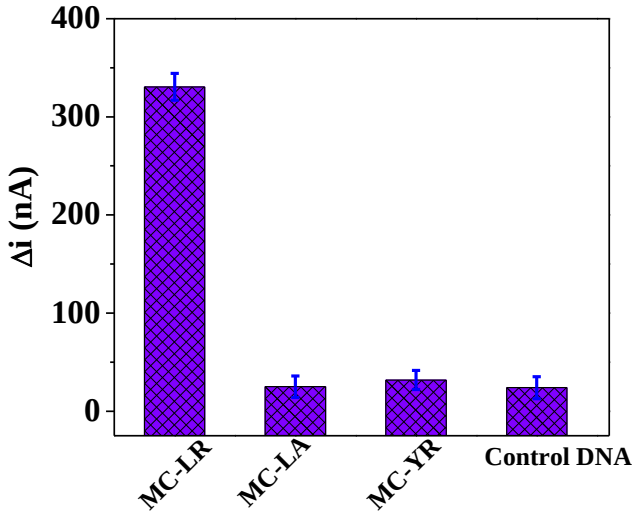

Highlights

- BiOBrNFs/NG p−n heterojunction was utilized as efficient PEC transducer.
- Photocurrent of BiOBrNFs/NG heterojunction was 4.6-fold higher than that of BiOBrNFs.
- The BiOBrNFs/NG was to immobilize the MC-LR aptamer for PEC analysis.
- The proposed method was used to detect MC-LR in fish samples.